Syntheses and characterizations of two silver(I) coordination polymers constructed from bipyrazole and dicarboxylate ligands

Xi-He Huang, Zu-Ping Xiao, Feng-Lan Wang, Ting Li, Meng Wen & Shu-Ting Wu

Taylor & Francis
Taylor & Francis Group

Syntheses and characterizations of two silver(I) coordination polymers constructed from bipyrazole and dicarboxylate ligands

XI-HE HUANG*†‡§ ⓘ , ZU-PING XIAO†, FENG-LAN WANG†, TING LI†, MENG WEN† and SHU-TING WU†

†College of Chemistry, Fuzhou University, Fuzhou, PR China
‡State Key Laboratory of Photocatalysis on Energy and Environment, Research Institute of Photocatalysis, Fuzhou, PR China
§State Key Laboratory of Structural Chemistry, Fujian Institute of Research on the Structure of Matter, Chinese Academy of Sciences, Fuzhou, PR China
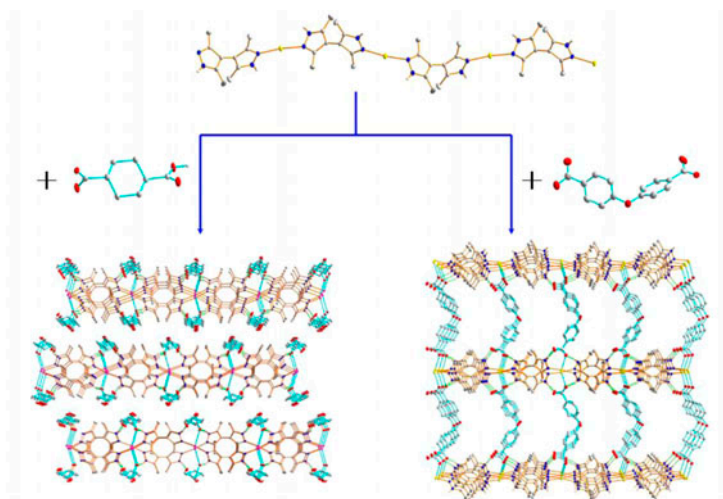
Two silver(I) compounds, $[Ag(H_2mbpz)(Hchda)]_n$ (**1**) and $[Ag_2(H_2mbpz)_2(oba)]_n$ (**2**) (where H_2mbpz = 3,3′,5,5′-tetramethyl-4,4′-bipyrazole, H_2chda = *trans*-cyclohexane-dicarboxylic acid and H_2oba = 4,4′-oxy-bis-benzoic acid), have been synthesized and characterized by single-crystal X-ray diffraction analyses. In both cases, the Ag(I) centers are linked by H_2mbpz ligands to form 1-D Ag (I)-H_2mbpz chains; then, the Ag(I)-$H_2mbpz$ chains connect with two neighboring congeners through Ag···Ag interactions, forming 2-D supramolecular layers. In **1**, the dicarboxylate is monodeprotonated and linked to form an anion chain through strong hydrogen bonding interaction. Such anion chains attach on two sides of the supramolecular layers via Ag–O bonds to form a neutral sandwich-like layered network. In **2**, the dicarboxylate is fully deprotonated and adopts a μ_2-$\eta1$:$\eta1$ mode to

---

*Corresponding author. Email: xhhuang@fzu.edu.cn

link two adjacent supramolecular layers to form a twofold interpenetrating 3-D supramolecular network. The thermal stability and luminescence of **1** were also studied.

Keywords: Coordination polymer; Silver(I); Bipyrazole; Dicarboxylate

1. Introduction

Synthesis of coordination polymers (CPs) is an active area of investigation owing to their potential as functional materials [1]. To predict the trend of assembly is a great challenge because assembly is influenced not only by the coordination bonds between the metal ions and ligands, but also by hydrogen bonding, $\pi \cdots \pi$ stacking and/or other weak supramolecular interactions [2]. Additionally, the assembly process is also affected by experimental factors, including temperature, pH, solvent, metal-to-ligand ratio, etc. [3]. There have been many attempts to probe the effects of experimental parameters on assembly of CPs [3], performing a series of reactions in similar conditions with only one factor varied, in which diversity among the assembly can be exclusively attributed to the change of this factor [4]. Some *in situ* studies of the assembly process for CPs on the molecular level shed light on the details of the CPs' crystal growth and nucleation mechanism [5]. However, fundamental information for the formation of CPs is still lacking because of the complex interplay of all these factors during the assembly process, which makes it difficult to predict and control the resulting structure [6]. Therefore, much more systematic work is required to understand how these factors relate to each other and affect the assembly process in the crystal engineering field.

Silver(I) ion has a closed shell d^{10} electronic configuration and can adopt diverse coordination numbers from 2 to 8, with no strong energetic preference for any particular geometry [7, 8]. Furthermore, the weak nature of the silver–ligand bond suggests that various supramolecular interactions, besides the experimental factors, may have influences on the structural formation of the final assemblies [8]. The geometrical flexibility of silver(I) coordination polyhedra may provide unique opportunities to construct architectures with desirable characteristics, and also offers a chance to explore the effects of a variety of factors on the formation of the resulting supramolecular assemblies.

Recently, we reported the syntheses and structures of four silver(I) CPs constructed from Ag(I)- 4,4′-bipyridine chains and chda^{2-} anions [9]. These studies show that the final structures are greatly affected by reaction factors, and such results are consistent with the various supramolecular interactions between the host and guest molecules within these compounds. As an expansion of our previous work on the structural chemistry of ternary silver(I) CPs consisting of dicarboxylate and bi-N-heterocyclic ligands, in this article, H$_2$mbpz was chosen as N-heterocyclic ligand, and H$_2$chda and H$_2$oba were selected as starting dicarboxylic acids. H$_2$mbpz has a variety of coordinated modes, such as bridging by using both pyrazole ends to bridge metal ions [10, 11]. Furthermore, the pyrazole can also be involved in hydrogen bond interactions, which might have a profound impact on the final structures of silver(I) CPs. Additionally, the obviously different configuration between the two dicarboxylic acids can also provide some clues on the supramolecular assemble through subsequent structural comparison. Herein, two new Ag(I) CPs, [Ag(H$_2$mbpz)(Hchda)]$_n$ (**1**) and [Ag$_2$(H$_2$mbpz)$_2$(oba)]$_n$ (**2**) were synthesized and their structures were determined by single-crystal X-ray diffraction

analyses. Additionally, **1** was characterized by elemental analysis, IR spectroscopy, and PXRD patterns. Thermogravimetric analysis (TG) and the luminescent properties of **1** have also been studied.

2. Experimental

2.1. *Materials and measurements*

All reagents were commercially available and used as received. $AgNO_3$ and Ag_2O were provided by Aladdin-reagent Inc. H_2chda was purchased from Acros-reagent Inc. and H_2oba and H_2mbpz were from Jinan Camolai Trading Company. The water used in all experiments was ultrapure. Elemental analyses of C, H, and N were carried out with a Vario EL III elemental analyzer. FT-IR spectra were recorded as KBr pellets from 4000 to 400 cm^{-1} on a Perkin–Elmer Spectrum 2000 FT-IR spectrometer. The fluorescence spectra were recorded on an Edinburgh Instrument F920 fluorescent spectrometer using an Xe lamp. Thermal analyses were performed on a Perkin–Elmer TGA7 instrument from room temperature to 700 °C with a heating rate of 10 °C min^{-1} under flowing nitrogen. Powder X-ray diffraction (PXRD) patterns were recorded with a MiniFlex–II X-ray diffractometer with Cu K_α radiation ($\lambda = 1.54178$ Å) at a scanning rate of 0.02° with 2θ ranging from 5 to 55°.

2.2. *Syntheses*

2.2.1. Preparation of $[Ag(H_2mbpz)(Hchda)]_n$ (1). A mixture of $AgNO_3$ (0.0169 g, 0.10 mM), H_2mbpz (0.0190 g, 0.10 mM), and H_2chda (0.0172 g, 0.10 mM) was stirred in 5 mL water, and then the resultant solution was heated in a 23 mL Teflon reactor at 140 °C for three days. After slow cooling to room temperature over a period of 24 h, pale yellow prism crystals of **1** in 58% yield (0.027 g) were obtained. Elemental analysis (%) calcd for $C_{18}H_{25}AgN_4O_4$: C, 46.07; H, 5.37; N, 11.94. Found: C, 46.41; H, 5.19; N, 11.79. IR (KBr pellet, cm^{-1}): 3396w, 3202s, 3166s, 3074s, 3012s, 2938vs, 2863s, 2820s, 1671s, 1627s, 1580m, 1552s, 1450m, 1421s, 1385m, 1358w, 1320m, 1311m, 1283m, 1260m, 1186m, 1137w, 1110w, 1071m, 1038m, 1016w, 911m, 903m, 793w, 779w, 731m, 709w, 689w, 634w, 543w, 516s.

2.2.2. Preparation of $[Ag_2(H_2mbpz)_2(oba)]_n$ (2). Compound **2** was synthesized in a similar way as for **1**, except that H_2chda is replaced by H_2oba (0.0258 g, 0.10 mM) and $AgNO_3$ replaced by Ag_2O (0.0116 g, 0.05 mM). Colorless block crystals were obtained; however, most of the crystalline products of **2** are contaminated by a black powder (mainly Ag, figure S6). Our limited attempts, including the optimization of reaction condition and several purification methods, for pure mass products of **2** were unsuccessful. The X-ray measurements of ten single crystals gained randomly from the mass products confirmed that the crystalline products are **2** exclusively.

Table 1. Crystallographic data and structural refinements for **1** and **2**.

Compound	**1**	**2**
Empirical formula	$C_{18}H_{25}AgN_4O_4$	$C_{34}H_{36}Ag_2N_8O_5$
Formula weight	469.29	852.45
Temperature (K)	293(2)	293(2)
Crystal system	Monoclinic	Monoclinic
Space group	$C2/c$	$C2/c$
a (Å)	9.416(2)	11.189(2)
b (Å)	18.735(5)	19.153(4)
c (Å)	22.799(6)	16.631(4)
α (°)	90	90
β (°)	96.832(3)	95.118(3)
γ (°)	90	90
V (Å^3)	3993.6(17)	3549.6(13)
Z	8	4
D_c (g^3 cm^{-3})	1.561	1.595
μ (mm^{-1})	1.040	1.155
F (0 0 0)	1920	1720
Crystal size (mm)	0.27 × 0.10 × 0.08	0.41 × 0.22 × 0.11
Theta range for data collection (°)	3.18–25.02	3.37–25.03
Reflections collected	13,878	12,280
Independent reflections	3523 [R_{int} = 0.0480]	3124 [R_{int} = 0.0281]
GOF on F^2	1.075	1.025
R_1, wR_2 [$I > 2\delta(I)$]	0.0479, 0.1019	0.0303, 0.0743
R_1, wR_2 [all data]	0.0524, 0.1044	0.0319, 0.0753
Largest diff. peak and hole (e Å^{-3})	0.640 and −0.380	0.512 and −0.296
CCDC number	949561	949562

Table 2. Selected bond lengths (Å) and angles (°) for **1** and **2**.

Compound **1**			
Ag(1)–N(1)	2.108(4)	Ag(1)–N(4)#1	2.097(4)
Ag(1)–O(1)	2.598(3)	Ag(1)···Ag(1)#2	2.9806(10)
C(17)–O(1)	1.249(5)	C(17)–O(2)	1.266(6)
C(18)–O(3)	1.296(6)	C(18)–O(4)	1.224(6)
N(4)#1–Ag(1)–N(1)	171.20(15)	N(4)#1–Ag(1)–O(1)	102.54(13)
N(1)–Ag(1)–O(1)	85.90(13)		
Symmetry codes: (#1) −x+1/2, y − 1/2, −z+1/2; (#2) −x, y, −z+1/2			

Compound **2**			
Ag(1)–N(1)#1	2.144(2)	Ag(1)–N(3)	2.133(2)
Ag(1)–O(1)	2.556(2)	Ag(1)···Ag(1)#2	3.0716(8)
C(17)–O(1)	1.260(4)	C(17)–O(2)	1.243(4)
N(3)–Ag(1)–N(1)#1	169.51(9)	N(3)–Ag(1)–O(1)	99.23(8)
N(1)#1–Ag(1)–O(1)	90.57(8)		
Symmetry codes: (#1) −x+1/2, y−1/2, −z+3/2; (#2) −x+1, y, −z+3/2			

2.3. *X-ray crystallography*

Suitable single crystals of **1** and **2** were mounted on glass fibers for X-ray measurement. Reflection data were collected at 293 K on a Rigaku Mercury CCD Saturn 724 diffractometer using graphite monochromated Mo K_α radiation (λ = 0.71073 Å). The data-sets were corrected for Lorentz and polarization factors, as well as by a numeric absorption correction method. All structures were solved by direct methods and refined by full matrix
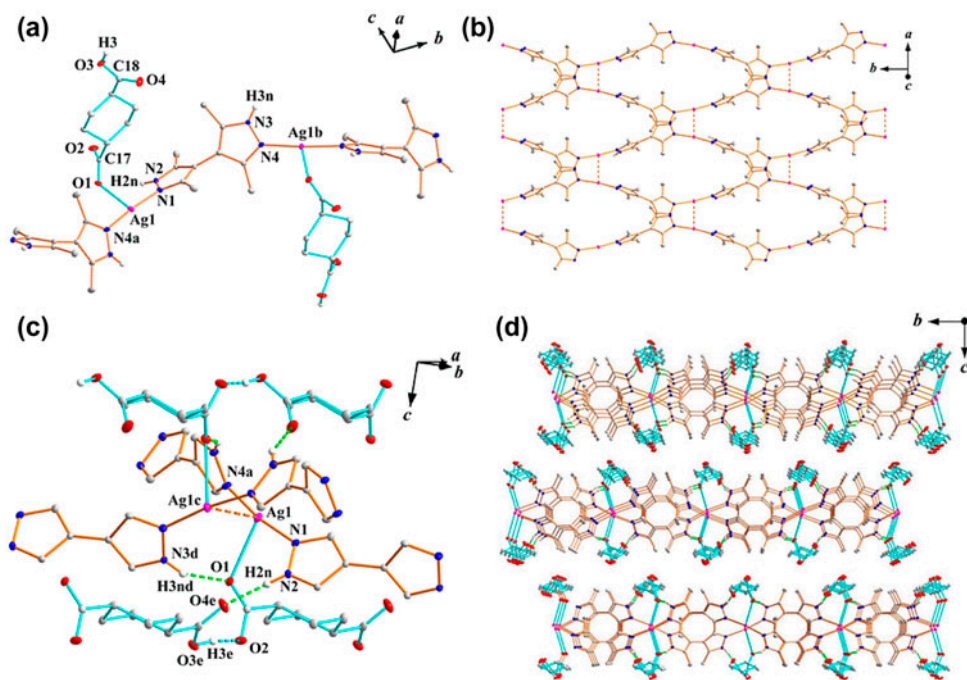
Figure 1. (a) View of the coordination environment of the Ag(I) ions with partial atom labeling in **1** and thermal ellipsoids at 30% probability. (b) View of the [Ag(H$_2$mbpz)]$_n$ supramolecular layer of **1** with Ag···Ag interactions. (c) Local structure of **1** showing the hydrogen bonded and Ag···Ag interactions. (d) Perspective view of **1** along the *a*-axis. Hydrogens bound to carbon are omitted for clarity. Symmetry codes: (a) $0.5 - x$, $-0.5 + y$, $0.5 - z$; (b) $0.5 - x$, $0.5 + y$, $0.5 - z$; (c) $-x, y, 0.5 - z$; (d) $-0.5 + x$, $-0.5 + y, z$; (e) $-1 + x, y, z$.

least-squares fitting on F^2 using the SHELX-97 program. All non-hydrogen atoms were refined with anisotropic thermal parameters. Hydrogens attached to C or N were positioned geometrically and treated as riding. The carboxylic hydrogen of **1** was located from difference Fourier maps and then restrained at fixed positions. All hydrogens were included in the structure factor calculation and refined isotropically. Crystal data and details of the data collection and the structure refinement are given in table 1. Selected bond lengths and angles are listed in table 2.

3. Results and discussion

3.1. *Crystal structures*

Single crystal X-ray diffraction reveals that **1** crystallizes in the monoclinic space group *C*2/*c* and the asymmetric unit contains one Ag(I), one neutral H$_2$mbpz ligand, and one Hchda$^-$ ligand. All atoms locate in general position. As shown in figure 1(a), Ag(I) is coordinated by two nitrogens from two H$_2$mbpz and one oxygen from Hchda$^-$, resulting in a near *T*-shaped geometry. The Ag–N bond lengths (2.097(4) and 2.108(4) Å) and the Ag–O bond length (2.598(3) Å) are well-matched to that of many similar compounds [7, 8]. However, the Ag–O

bond length is obviously longer than some reported Ag(I) carboxylates, implying a weak Ag–O interaction. The dihedral angle between the ring planes of the pyrazole groups of H_2mbpz is 62.34(15)°. The H_2mbpz ligands bridge the Ag(I) ions alternately into an infinite [Ag(H_2mbpz)]$_n$ right-handed helical chain extending along the b axis. Such right-handed helixes further link with two adjacent helixes with identical handedness through Ag···Ag interactions, forming a chiral 2-D supramolecular [Ag(H_2mbpz)]$_n$ network lying on crystallographic ab plane [figure 1(b)]. The Ag···Ag separation of 2.9806(10) Å is shorter than the *van der Waals* contact distance (3.44 Å) for Ag–Ag, indicating the argentophilic interactions.

There are strong hydrogen-bonded interactions between the Hchda$^-$ anions [see table S1 for details (see online supplemental material at http://dx.doi.org/10.1080/00958972.2015. 1022165)], forming an anion chain propagating along the a-axis [figure 1(c)]. The O(3e)···O (2) distance of 2.483(5) Å indicates the existence of an anion association between two adjacent carboxylic groups. As shown in figure 1(d), these Hchda$^-$ anion chains attach on two sides of the 2-D [Ag(H_2mbpz)]$_n$ layer via Ag–O bonds involving O(1) from the deprotonated carboxylic groups, resulting in a neutral sandwich-like 2-D layered network. These layers further stack alternately in an ···ABAB··· fashion with inverse relation, giving the centrosymmetric structure of **1**. Furthermore, H-bonding interactions are observed between the pyrazole groups as H-donors and the carboxylic O as acceptors within the sandwich-like layer (N(2)–H(2 N)···O(4) and N(3)-H(3 N)···O(1), see table S1 for details). No π–π stacking interaction or inter-layered H-bonding contact is found in the structure of **1**.
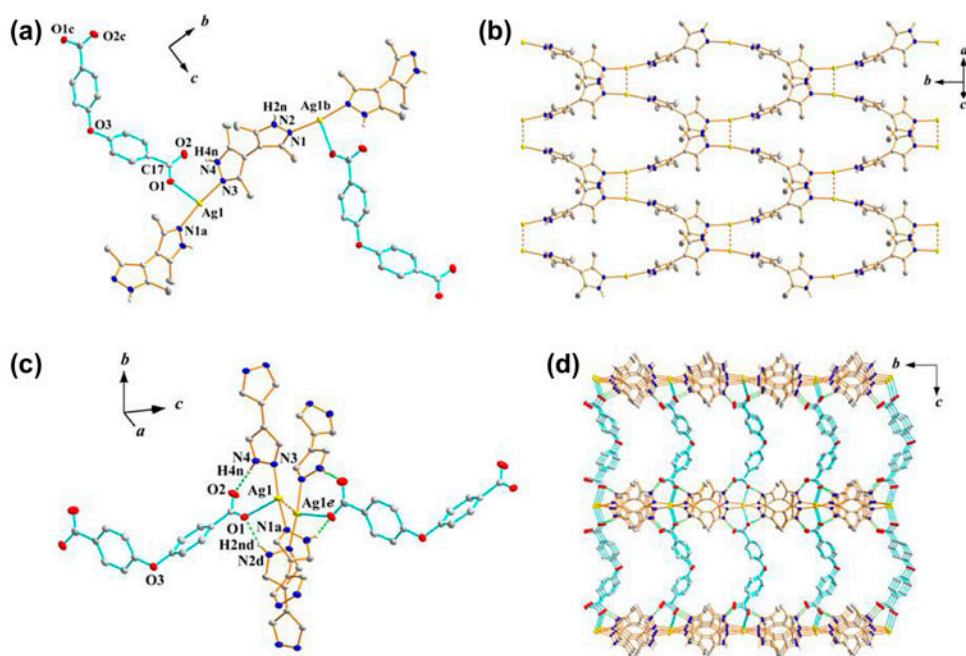

Figure 2.   (a) View of the coordination environment of the Ag(I) ions with partial atom labeling in **2** and thermal ellipsoids at 30% probability. (b) View of the [Ag(H_2mbpz)]$_n$ supramolecular layer of **2** through Ag···Ag interactions. (c) Local structure of **2** showing the hydrogen bond and Ag···Ag interactions. (d) Perspective view of **2** along the a-axis. Hydrogens bound to carbon and partial methyl groups are omitted for clarity. Symmetry codes: (a) $0.5 - x$, $-0.5 + y$, $1.5 - z$; (b) $0.5 - x$, $0.5 + y$, $1.5 - z$; (c) $1 - x$, y, $0.5 - z$; (d) $0.5 + x$, $-0.5 + y$, z; (e) $1 - x$, y, $1.5 - z$.

From the viewpoint of topology, each dimeric Ag–Ag unit can be considered as a six-connected node, which connects with four adjacent nodes through H_2mbpz ligands and two other nodes via double $Hchda^-$ anionic chains up and down. Thus, the 2-D layered network can be described as a hexagonal lattice, i.e. a uninodal six-connected *hxl* topology with a *Schlafli* symbol of 3^6 (figure S3).

Compound **2** also crystallizes in the monoclinic space group $C2/c$ and its asymmetric unit contains one Ag(I), one H_2mbpz ligand, and a half of oba^{2-}. The O(3) of the oba^{2-} lies on a crystallographic twofold rotation axis and other atoms locate in general positions. As shown in figure 2(a), both Ag(I) and H_2mbpz adopt identical coordination mode to **1**, i.e. a near *T*-shaped geometry for Ag(I) ion, and μ_2-$\eta1$:$\eta1$ connected mode for H_2mbpz, to form a similar $[Ag(H_2mbpz)]_n$ right-handed helical chain extending along the *b* axis. The Ag–N bond lengths (2.133(2) and 2.144(2) Å) are somewhat longer than that of **1**, while the Ag–O bond (2.556(2) Å) is a little shorter than its analog in **1**. The torsion angle of H_2mbpz (65.23(10)°) is compared with that of **1**. Similar to **1**, the Ag-H_2mbpz right-handed helices of **2** also link with two adjacent right-handed helices through Ag···Ag interactions to form a chiral 2-D supramolecular layer parallel to the crystallographic *ab* plane [figure 2(b)]. The Ag···Ag separation of 3.0716(8) Å is longer than that in **1**, however, is still shorter than the *van der Waals* contact distance for Ag–Ag, implying the presence of argentophilic interactions.

There are great differences of the connect modes between the dicarboxylate and $[Ag(H_2mbpz)]_n$ layers of **1** and **2**. As shown in figure 2(c) and (d), oba^{2-} adopts μ_2-$\eta1$:$\eta1$ to link two 2-D Ag-H_2mbpz layers into a 3-D supramolecular framework. Such 3-D framework is chiral and its empty space is filled by another central symmetry relative analog. Thus, the structure of **2** can be described as a twofold interpenetrated supramolecular *pcu* network (figure S4), where the dimeric Ag–Ag unit is simplified as a six-connected node. Again, there are only intra-framework H-bonding interactions between the pyrazole groups and the carboxylic group, (N(2)–H(2 N)···O(1) and N(4)–H(4 N)···O(2), see table S1 for details). And no π–π stacking interaction or inter-framework H-bonding contacts can be observed in **2**.

3.2. Structural comparison

Although H_2mbpz had been widely employed to construct the CPs or metal-organic frameworks, only a few silver(I) CPs consisting of H_2mbpz ligand have been reported [11]. For example, Zhang *et al.* reported several porous silver(I) CPs with trigonal $\{Ag_3(mbpz)_3\}$ clusters, in which the mbpz ligand is full-deprotonated and adopts μ_4-$\eta1$:$\eta1$:$\eta1$:$\eta1$ mode to connect four silver(I) centers [11a, b]. Domasevitch *et al.* reported a series of silver(I) CPs showing a variety of helical architectures with double helicates $Ag(H_2mbpz)$. All H_2mbpz ligands in such double helicates are bridging neutral group, connecting two silver(I) ions. The counterions, such as NO_3^-, ClO_4^-, $CF_3SO_3^-$, and $C_2F_5CO_2^-$, act as bridge ligands supporting the double helices or as terminal ligands suspending $Ag(H_2mbpz)$ chains [11c]. In this study, as detailed above, the H_2mbpz ligands uniformly are bidentate spacers to connect the Ag(I) centers into $[Ag(H_2mbpz)]_n$ helices of **1** and **2**, and thus, their structural discrepancy should be mainly attributed to the choice of the different dicarboxylates. Although the structure of the $[Ag(H_2mbpz)]_n$ supramolecular layer of **1** is similar to that of **2**, there is obvious difference between the distance interval of the medial axis of the $[Ag(H_2mbpz)]_n$ helices (about 4.708 and 5.595 Å for **1** for **2**, respectively, half the length of the *a*-axis) (figure 3).
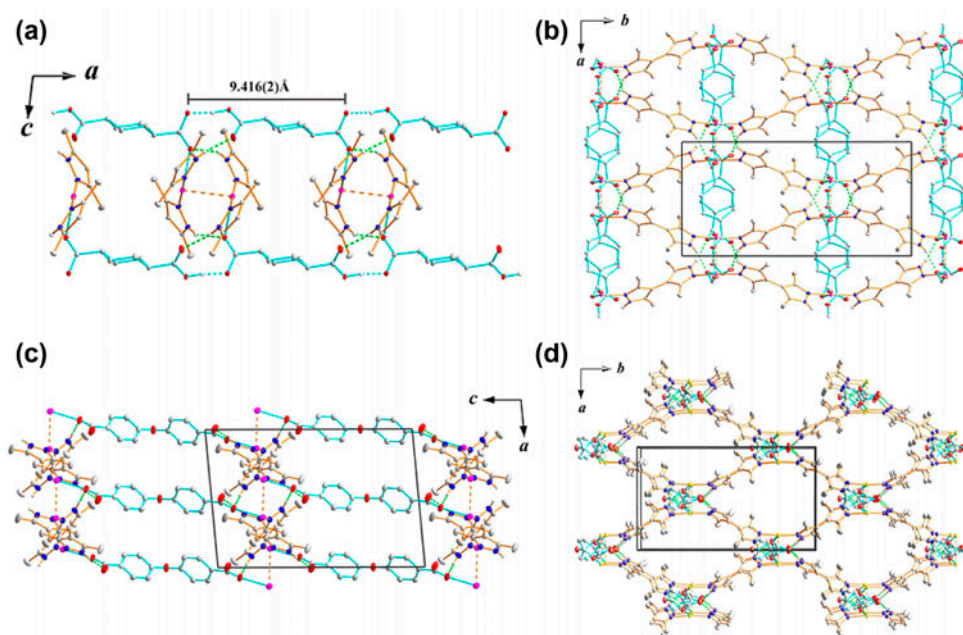
Figure 3. (a) The sandwich-like layered network view of **1** along the *b*-axis, showing the Hchda⁻ anion chains connected by O–H⋯O strong hydrogen bonds. The distance of the repeated unit of the Hchda⁻ anion chain is marked. (b) The sandwich-like layered network view of **1** along the *c*-axis. (c) Packing diagram of **2** viewed along the *b*-axis. (d) 3-D supramolecular framework of **2** viewed along the *c*-axis.

Such structural distinction indicates that the $[Ag(H_2mbpz)]_n$ helices can readily modulate their inter-chain distance through changing the Ag–O bonds, Ag⋯Ag interaction, and hydrogen bonds for different dicarboxylate anions [figures 1(c), 2(c) and table 2]. As shown in figure 3(a), the *a*-axis length of **1** depends on the distance of the repeat unit of the Hchda⁻ anion chain. Because of the obvious geometrical difference between Hchda⁻ and oba²⁻ ions, a distinct connection mode between the $[Ag(H_2mbpz)]_n$ chains and oba²⁻ ions is adopted in **2**, resulting in the 3-D supramolecular framework [figure 2(d)]. The longer *a*-axis length of **2** gives its larger 1-D channel to accommodate another supramolecular framework [figure 3(d)].

The deprotonation degree and coordination mode of dicarboxylate ligand within **1** is different from **2**. We speculate that the pH value of the solution plays an important role on their structure. However, our limited attempts for the syntheses of more ternary Ag(I)/ H_2mbpz CPs, such as that with chda²⁻ or Hoba⁻ anions, under various pH values (within about 2–7 through adding NaOH or HNO_3 solution) and Ag(I) resource ($AgNO_3$ or Ag_2O) as starting materials were unsuccessful. These experiments also indicate that there are intrinsic structural factors impacting the formation of **1** and **2**, and an appropriate reaction condition is needed for the assembly process. Thus, structural and experimental results show that there might be a two-step route during the assembly processes in each case, i.e. the [Ag $(H_2mbpz)]_n$ helices are created first, and then the helices link with each other through ligand-unsupported Ag⋯Ag interactions, hydrogen bonds and weak Ag–O bonds with dicarboxylate anions to form the final architectures of **1** and **2**.
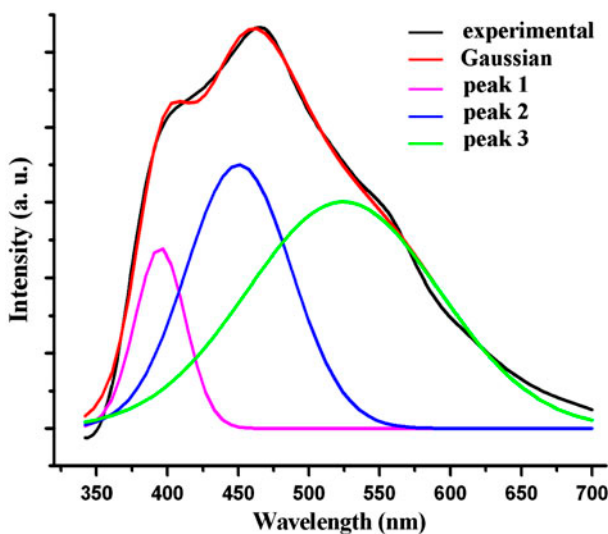
Figure 4. Photoluminescence curve of **1**. The Gaussian fit curve showing three emission peaks.

3.3. *Properties*

3.3.1. Powder XRD studies. PXRD has been used to verify the phase purity of the synthesized samples in the solid state (figure S1). The experimental PXRD patterns correspond well with the simulated patterns generated from the results of the single crystal data, indicative of pure products. The dissimilarities in intensity may be due to preferred orientation of the powder samples during the collection of the experimental PXRD data.

3.3.2. Thermogravimetric analysis. The TG analysis of **1** was performed under N_2 and the TG curve and is shown in figure S5. The TG curve of **1** shows that the first weight loss of 17.1% at 200–265 °C corresponds to loss of cyclohexane fragment from Hchda (Calcd: 17.1%). The second weight loss of 38.3% from 265 to 360 °C is attributed to loss of H_2mbpz (calcd: 41.0%). The succeeding weight loss of 19.4% from 360 to 540 °C accompanies the release of the carboxyl fragment decomposing from Hchda (calcd: 19.2%). The residual weight of 23.8% is consistent with that of 24.7% calculated for Ag_2O.

3.3.3. Photoluminescence. Photoluminescence of **1** was performed at room temperature in the solid state (figure 4). The broad emission with maximum at 468 nm and a shoulder at 402 nm was observed upon excitation by 340 nm. However, the Gaussian fit curve shows that such photoluminescence curve contains three emission peaks at 395, 450, and 525 nm. Obviously, these emission bands with emission maxima at 395 and 450 nm can be ascribed to ligand centered $\pi \rightarrow \pi^*$ transitions for Hchda and H_2mbpz, respectively [13]. The low-energy emission peaks at 525 nm should come from the p–π^* to Ag-4d charge transfer (MLCT) [9]. The luminescent decay profile of **1** can be fitted with a double-exponential decay function with $\tau_1 = 0.56\ \mu s$ (37%), $\tau_2 = 8.54$ ns (63%). The long emission lifetimes

could be assigned to ligand-to-metal charge-transfer triplet excited states (^{3}[MLCT]) mentioned above.

4. Conclusion

Two silver(I) CPs based on bipyrazole and different dicarboxylates have been synthesized and characterized. The two compounds display versatile coordination features with 2-D and 3-D supramolecular networks. The structural and experimental results show that there might be a two-step route during assembly of the ternary Ag(I)/H$_2$mbpz/dicarboxylate system. The Ag(I)-H$_2$mbpz helical chain is produced in the first assembly step and the formed [Ag(H$_2$mbpz)]$_n$ helices can readily modulate their inter-chain distance through changing the Ag–O bonds, Ag···Ag interaction, and hydrogen bonds involving the dicarboxylate anions in the second assembly step to form the final architectures of **1** and **2**. In addition, **1** displays modest thermal stability and interesting solid-state fluorescent emission.

Supplementary material

X-ray crystallographic data in *cif* format; figures S1–S6 for the simulated and experimental PXRD patterns, and infrared spectrum of **1**, and the topology pictures for **1** and **2**, TG curve for **1**; table S1 for hydrogen bond geometries for **1** and **2**.

Disclosure statement

No potential conflict of interest was reported by the authors.

ORCID

Xi-He Huang http://orcid.org/0000-0003-0469-4284

References

[1] (a) X.-C. Shan, F.-L. Jiang, D.-Q. Yuan, H.-B. Zhang, M.-Y. Wu, L. Chen, J. Wei, S.-Q. Zhang, J. Pan, M.-C. Hong. *Chem. Sci.*, **4**, 1484 (2013); (b) M. O'Keeffe, O.M. Yaghi. *Chem. Rev.*, **112**, 675 (2012); (c) J.-P. Zhang, Y.-B. Zhang, J.-B. Lin, X.-M. Chen. *Chem. Rev.*, **112**, 1001 (2012); (d) V. Bulach, F. Sguerra, M.W. Hosseini. *Coord. Chem. Rev.*, **256**, 1468 (2012); (e) G.Y. Jiang, T. Wu, S.-T. Zheng, X. Zhao, Q.P. Lin, X.H. Bu, P.Y. Feng. *Cryst. Growth Des.*, **11**, 3713 (2011); (f) K. Biradha, C.-Y. Su, J.J. Vittal. *Cryst. Growth Des.*, **11**, 875 (2011); (g) X.-J. Kong, L.-S. Long, Z. Zheng, R.-B. Huang, L.-S. Zheng. *Acc. Chem. Res.*, **43**, 201 (2010).

[2] (a) Q.-B. Bo, H.-Y. Wang, D.-Q. Wang. *New J. Chem.*, **37**, 380 (2013); (b) R. Chakrabarty, P.S. Mukherjee, P.J. Stang. *Chem. Rev.*, **111**, 6810 (2011); (c) W.H. Zhang, Z. Dong, Y.Y. Wang, L. Hou, J.C. Jin, W.H. Huang, Q.Z. Shi. *Dalton Trans.*, **40**, 2509 (2011); (d) C. Carpanese, S. Ferlay, N. Kyritsakas, M. Henry, M.W. Hosseini. *Chem. Commun.*, **44**, 6786 (2009); (e) L. Ma, W. Lin. *J. Am. Chem. Soc.*, **130**, 13834 (2008).

[3] (a) H.Q. Zheng, L. Xing, Y.Y. Cao, S.A. Che. *Coord. Chem. Rev.*, **257**, 1933 (2013); (b) G.-P. Yang, L. Hou, L.-F. Ma, Y.-Y. Wang. *CrystEngComm*, **15**, 2561 (2013); (c) P. Cui, L. Ren, Z. Chen, H. Hu, B. Zhao, W. Shi, P. Cheng. *Inorg. Chem.*, **51**, 2303 (2012); (d) F. Song, C. Wang, J.M. Falkowski, L. Ma, W. Lin. *J. Am. Chem. Soc.*, **132**, 15390 (2012); (e) Y.-Q. Lan, H.-L. Jiang, S.-L. Li, Q. Xu. *Inorg. Chem.*, **51**, 7484 (2012); (f) M. Chen, Y. Lu, J. Fan, G.-C. Lv, Y. Zhao, Y. Zhang, W.-Y. Sun. *CrystEngComm*, **14**, 2015 (2012).

[4] (a) S.-T. Wu, L.-S. Long, R.-B. Huang, L.-S. Zheng. *Cryst. Growth Des.*, **7**, 1746 (2007); (b) U. Kumar, J. Thomas, N. Thirupathi. *Inorg. Chem.*, **49**, 62 (2010); (c) L.-J. Li, C. Qin, X.-L. Wang, S. Wang, L. Zhao, G.-S. Yang, H.-N. Wang, G. Yuan, K.-Z. Shao, Z.-M. Su. *CrystEngComm*, **14**, 124 (2012).

[5] (a) O. Shekhah, H. Wang, D. Zacher, R.A. Fischer, C. Wöll. *Angew. Chem. Int. Ed.*, **48**, 5038 (2009); (b) M. Haouas, C. Volkringer, T. Loiseau, G. Férey, F. Taulelle. *Chem. Mater.*, **24**, 2462 (2012).

[6] (a) Y. Tao, J.-R. Li, Z. Chang, X.-H. Bu. *Cryst. Growth Des.*, **10**, 564 (2010); (b) S. Upreti, A. Datta, A. Ramanan. *Cryst. Growth Des.*, **5**, 966 (2007); (c) Y.-W. Li, H. Ma, Y.-Q. Chen, K.-H. He, Z.-X. Li, X.-H. Bu. *Cryst. Growth Des.*, **12**, 189 (2012).

[7] (a) D. Sun, Z.-H. Wei, C.-F. Yang, D.-F. Wang, N. Zhang, R.-B. Huang, L.-S. Zheng. *CrystEngComm*, **13**, 1591 (2011); (b) A. Karmakar, H.M. Titi, I. Goldberg. *Cryst. Growth Des.*, **11**, 2621 (2011); (c) G.-P. Yang, J.-H. Zhou, Y.-Y. Wang, P. Liu, C.-C. Shi, A.-Y. Fu, Q.-Z. Shi. *CrystEngComm*, **13**, 33 (2011); (d) X.-Q. Fang, Z.-P. Deng, L.-H. Huo, W. Wan, Z.-B. Zhu, H. Zhao, S. Gao. *Inorg. Chem.*, **50**, 12562 (2011); (e) N.C. Kasuga, R. Yoshikawa, Y. Sakai, K. Nomiya. *Inorg. Chem.*, **51**, 1640 (2012); (f) X.-F. Kuang, X.-Y. Wu, R.-M. Yu, J.P. Donahue, J.-S. Huang, C.-Z. Lu. *Nat. Chem.*, **2**, 461 (2010); (g) X.-L. Chen, Y.-L. Qiao, L.-J. Gao, M.-L. Zhang. *J. Coord. Chem.*, **66**, 3749 (2013); (h) J.-C. Jin, N.-N. Yan, W.-G. Chang, J.-Q. Liu, Z.-C. Yin, G.-N. Xu, K.-F. Yue, Y.-Y. Wang. *J. Coord. Chem.*, **66**, 3509 (2013); (i) A. Karmakar, I. Goldberg. *CrystEngComm*, **13**, 350 (2011).

[8] (a) G.F. Swiegers, T.J. Malefetse. *Chem. Rev.*, **100**, 3483 (2000); (b) J.-C. Jin, Y.-Y. Wang, W.-H. Zhang, A.S. Lermontov, E.K. Lermontova, Q.-Z. Shi. *Dalton Trans.*, **38**, 10181 (2009).

[9] T. Li, X.-H. Huang, Y.-F. Zhao, H.-H. Li, S.-T. Wu, C.-C. Huang. *Dalton Trans.*, **41**, 12872 (2012).

[10] (a) L. Hou, Y.Y. Lin, X.M. Chen. *Inorg. Chem.*, **47**, 1346 (2008); (b) J. He, Y.G. Yin, T. Wu, D. Li, X.C. Huang. *Chem. Commun.*, 2845 (2006); (c) L.N. Jia, Y. Zhao, L. Hou, L. Cui, H.H. Wang, Y.Y. Wang. *J. Solid State Chem.*, **210**, 251 (2014).

[11] (a) J.P. Zhang, S. Horike, S. Kitagawa. *Angew. Chem. Int. Ed.*, **46**, 889 (2007); (b) J.P. Zhang, S. Kitagawa. *J. Am. Chem. Soc.*, **130**, 907 (2008); (c) K.V. Domasevitch, I. Boldog, E.B. Rusanov, J. Hunger, S. Blaurock, M. Schröder, J. Sieler. *Z. Anorg. Allg. Chem.*, **631**, 1095 (2005).

[12] (a) H. Fei, U.L. Paw, D.L. Rogow, M.R. Bresler, Y.A. Abdollahian, S.R.J. Oliver. *Chem. Mater.*, **22**, 2027 (2010); (b) M.-S. Wang, S.-P. Guo, Y. Li, L.-Z. Cai, J.-P. Zou, G. Xu, W.-W. Zhou, F.-K. Zheng, G.-C. Guo. *J. Am. Chem. Soc.*, **131**, 13572 (2009).

[13] (a) B.F. Huang, T. Sun, Z. Sharifzadeh, M.Y. Lv, H.P. Xiao, X.H. Li, A. Morsali. *Inorg. Chim. Acta*, **405**, 83 (2013); (b) L.Y. Du, W.J. Shi, L. Hou, Y.-Y. Wang, Q.Z. Shi, Z.H. Zhu. *Inorg. Chem.*, **52**, 14018 (2013).